# Redox conversion of cobalt(II)-diselenide to cobalt(III)-selenolate compounds: comparison with their sulfur analogs

Marvelous, C.; Azevedo Santos, L. de; Siegler, M.A.; Fonseca Guerra, C.; Bouwman, E.

EurJIC
European Journal of Inorganic Chemistry

Research Article
doi.org/10.1002/ejic.202200445

Chemistry Europe
European Chemical Societies Publishing

www.eurjic.org



# Redox Conversion of Cobalt(II)-Diselenide to Cobalt(III)-Selenolate Compounds: Comparison with Their Sulfur Analogs

Christian Marvelous,[a] Lucas de Azevedo Santos,[b] Maxime A. Siegler,[c] Célia Fonseca Guerra,*[a, b] and Elisabeth Bouwman*[a]

The synthesis of the selenium-based ligand $L^1SeSeL^1$ (2,2′-diselanediylbis(N,N-bis(pyridin-2-ylmethyl)ethan-1-amine) is described along with its reactivity with cobalt(II) salts. The cobalt(II)-diselenide complex $[Co_2(L^1SeSeL^1)Cl_4]$ was obtained in good yield, and its spectroscopic properties closely resemble that of its sulfur analog. Reaction of $L^1SeSeL^1$ with Co(II) thiocyanate results in the formation of the cobalt(III) compound $[Co(L^1Se)(NCS)_2]$, similar to reaction of $L^1SSL^1$. The redox-conversion reactions from the Co(II)-diselenide compound $[Co(L^1SeSeL^1)Cl_4]$ using external triggers such as removal of the halide ions or the addition of the strong-field ligand 8-quinolinolate resulted in good yields of the Co(III)-selenolate complexes $[Co(L^1Se)(MeCN)_2](SbF_6)_2$ and $[Co(L^1Se)(quin)]Cl$. Our computational studies show that the ligand-field splitting energy of the selenium compounds is smaller than their sulfur analogs, indicating that redox-conversion of cobalt(II)-diselenide to cobalt(III)-selenolate complexes may be more arduous than that for the related sulfur compounds.

## Introduction

Electron-transfer reactions frequently occur in biological systems, usually involving transition-metal ions in metalloenzymes.[1] Among these biological systems, selenium is used in biomimetic studies as an analog for sulfur, as selenium is present in nature in the amino acid selenocysteine, often resulting in enhanced reaction rates compared to cysteine-containing enzymes.[2] The redox chemistry of selenium compounds is known to be similar to their sulfur analogues, for example the reduction of the diselenide bond into selenolate ions. Additionally, selenium compounds can participate in faster thiol/disulfide-like exchange reactions,[3] which is an indirect consequence of the more nucleophilic properties of selenium under neutral conditions.[4]

In the past decade, the redox-conversion of metal-thiolate and metal-disulfide compounds has gathered a lot of interest. In this reaction electrons of two low-valent metal centers are transferred to a disulfide group, thereby creating two metal centers in a high oxidation state and two thiolate ions. The study of the redox-conversion of thiolate and disulfide compounds may provide mechanistic understanding on electron-transfer reactions catalyzed by metalloenzymes. Some reported examples concern the redox-conversion of copper(I)-disulfide vs copper(II)-thiolate complexes and cobalt(II)-disulfide vs cobalt(III)-thiolate complexes.[5] The redox-conversion of cobalt(II)-disulfide to cobalt(III)-thiolate is particularly interesting for several reasons. First of all, only few examples have been reported on this matter and expansion of the scope will be helpful to gain more understanding. Additionally, the reactivity of specific disulfide ligands is a point of interest as slightly different ligands may result in different outcomes. For example, the ligand $L^1SSL^1$ upon reaction with $Co(SCN)_2$ yields a cobalt(III)-thiolate complex,[5b] whereas the same reaction with the dimethylated ligand $L^2SSL^2$ leads to formation of a cobalt(II)-disulfide complex (Scheme 1).[6] Finally, the redox-conversion reaction mechanism seems to be different for the cobalt-based system than for the copper-based system.[5b,6–7] The reactivity of the cobalt-based systems with both of these disulfide ligand scaffolds has been reported.[6,8] It was found that the ligand-field strength of the exogenous ligand affects the formation of cobalt(III)-thiolate complexes. In addition, the mechanism of the redox-conversion reaction appeared to depend on the different coordination modes of the disulfide ligand as well as the exogenous bidentate ligand.[8–9]

To the best of our knowledge, the redox-conversion reaction using selenium-based ligands has not yet been

[a] Dr. C. Marvelous, Prof. Dr. C. Fonseca Guerra, Prof. Dr. E. Bouwman
Leiden Institute of Chemistry
Leiden University
P.O. Box 9502, 2300 RA Leiden, The Netherlands
E-mail: c.fonsecaguerra@vu.nl
bouwman@lic.leidenuniv.nl
[b] Dr. L. de Azevedo Santos, Prof. Dr. C. Fonseca Guerra
Department of Theoretical Chemistry, Amsterdam Center for Multiscale Modelling (ACMM)
Vrije Universiteit Amsterdam
De Boelelaan 1083, 1081 HV Amsterdam, The Netherlands
[c] Dr. M. A. Siegler
Department of Chemistry
Johns Hopkins University
3400 N. Charles Street, Baltimore, Maryland 21218, United States

Supporting information for this article is available on the WWW under https://doi.org/10.1002/ejic.202200445

Part of a joint Special Collection with ChemCatChem and EurJOC on the Netherlands Institute for Catalysis Research. Please click here for more articles in the collection.

Research Article
doi.org/10.1002/ejic.202200445



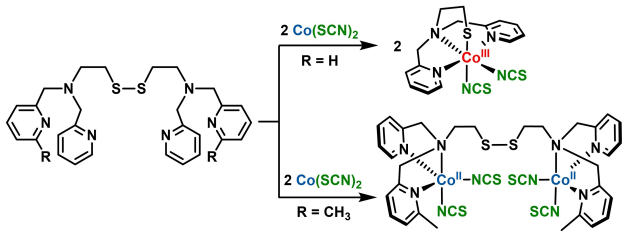


**Scheme 1.** Different reactivity of ligand $L^1SSL^1$ (R=H) and $L^2SSL^2$ ($R=CH_3$) with $Co(SCN)_2$.[10,11]

reported. It is of importance to know whether redox conversion can also occur with selenolate/diselenide species, as it may give rise to a new perspective on the importance of selenium compared to sulfur in electron-transfer reactions in biology. Yet, the use of selenium as a replacement for sulfur in the redox-conversion reaction of Co(II)-diselenide to the corresponding Co(III)-selenolate complex may be challenging. The diselenide bond has been reported to be more stable towards reduction than the disulfide bond,[10] and thus would make the redox-conversion reaction more complicated. Therefore, it is our interest to investigate the redox-conversion reaction of the selenium-based ligand $L^1SeSeL^1$ by the reaction with different cobalt(II) salts or adjusting the ligand-field strength with use of external ligands.

## Results and Discussion

### Synthesis of the Compounds

The precursor of the ligand, selenocystamine dihydrochloride, was obtained in 37% yield as a light yellow powder and characterized using ESI-MS and $^1$H-NMR (Figure S1 and Figure S2). The ligand 2,2′-diselanediylbis(N,N-bis(pyridin-2-ylmethyl)ethan-1-amine) ($L^1SeSeL^1$) was prepared via the reductive

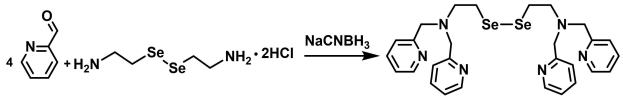


**Scheme 2.** Synthesis scheme of ligand $L^1SeSeL^1$.

amination of selenocystamine dihydrochloride with 2-pyridinecarboxaldehyde using sodium cyanoborohydride as reducing agent (Scheme 2). The ligand $L^1SeSeL^1$ was obtained as a pale red solid in 26% yield after recrystallization. The ESI-MS spectrum (Figure S3) shows peaks at *m/z* 612.9 and 306.8 corresponding to the species $[L^1SeSeL^1+H]^+$ and $[L^1SeSeL^1+2H]^{2+}$, respectively. Both $^1$H-NMR spectroscopy (Figure S4) and elemental analysis showed that the ligand $L^1SeSeL^1$ was obtained analytically pure.

Addition of the ligand $L^1SeSeL^1$ to a solution containing two equivalents of $CoCl_2$ in acetonitrile afforded a dark purple solution of the diselenide compound $[Co_2(L^1SeSeL^1)(Cl)_4]$ ([**1**]) (Scheme 3). Compound [**1**] was isolated as a purple solid in 50% yield. An ESI-MS spectrum of the purple powder dissolved in acetonitrile (Figure S5) shows peaks at *m/z* 845.1 and 400.0 corresponding to the species $[\mathbf{1} - 2Cl^- + HCOO^-]^+$ and $[\mathbf{1} - 2Cl^-]^{2+}$, respectively, showing distinct isotopic distributions due to the presence of selenium in the compound. The presence of two high-spin cobalt(II) ions in [**1**] is indicated by the value of the magnetic moment of 5.98 $\mu_B$, calculated for the dinuclear compound. The $^1$H-NMR spectrum of [**1**] in $CD_3CN$ (Figure S6) shows peaks in the region between −8.64 ppm up to 88.34 ppm due to the paramagnetic nature of the compound. Compound [**1**] was proven to be analytically pure by elemental analysis and its structure was further elucidated using single crystal X-ray diffraction.

The cobalt(III)-selenolate compound $[Co(L^1Se)(NCS)_2]$ ([**2**]) was obtained from a reaction of the ligand $L^1SeSeL^1$ with two equivalents of $Co(SCN)_2$, while the compounds $[Co(L^1Se)(MeCN)_2](SbF_6)_2$ ([**3**]$(SbF_6)_2$) and $[Co(L^1Se)(quin)]Cl$ ([**4**]Cl)

Elisabeth Bouwman is Professor of Inorganic Chemistry at the Leiden Institute of Chemistry at Leiden University in the Netherlands. She received her PhD (1990) degree from Leiden University, studying under supervision of Jan Reedijk. She carried out postdoctoral research at the Technical University Delft (the Netherlands) and Indiana University in Bloomington (IN, USA) and returned to Leiden University as a faculty member in 1991. Her research interests concern biomimetic inorganic chemistry and the development of homogeneous catalysts for novel types of reactions.

Célia Fonseca Guerra is Professor of Supramolecular Quantum Biochemistry at the Vrije Universiteit Amsterdam in the Netherlands. She received her PhD degree (2000) from Vrije Universiteit Amsterdam under supervision of Evert Jan Baerends and Jaap Snijders. She has been NRSC-C Postdoctoral Associate at the Vrije Universiteit Amsterdam and visiting scientist at the University of Girona. In 2013 she was visiting Professor at Warsaw University of Technology in Poland and from 2017 till 2022 Extraordinary Professor of Applied Theoretical Chemistry at Leiden University. Her research focuses on understanding chemical interactions in self-assembly of biological and supramolecular systems with Kohn-Sham Molecular Orbital theory and implementing design principles from computational investigations.

Research Article
doi.org/10.1002/ejic.202200445

Chemistry Europe
European Chemical Societies Publishing

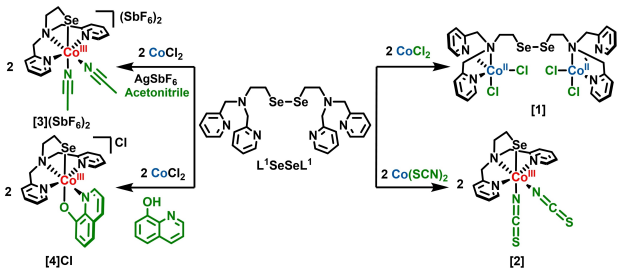


**Scheme 3.** Synthesis scheme of the complexes described in this manuscript.

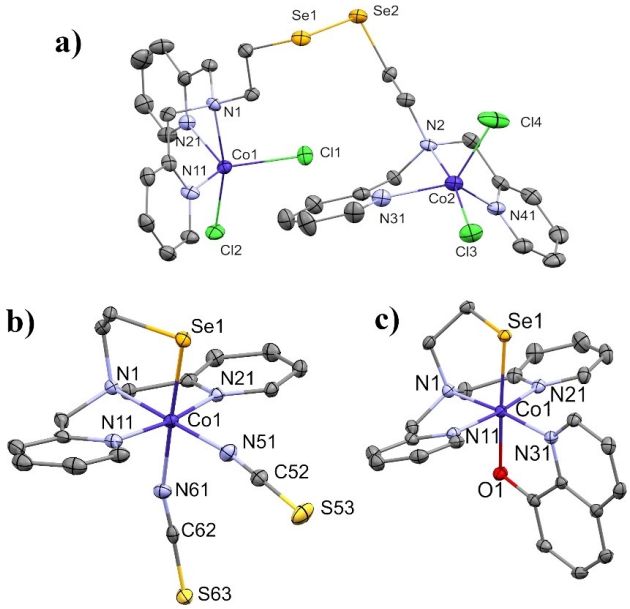


**Figure 1.** Displacement ellipsoid plots (50 % probability level) of a) $[Co_2(L^1SeSeL^1)Cl_4]$ ([**1**]), b) $[Co(L^1Se)(NCS)_2]$ ([**2**]), and c) $[Co(L^1Se)(quin)]^+$ ([**4**]$^+$) at 110(2) K. Hydrogen atoms, non-coordinated anions, and lattice solvent molecules are omitted for clarity.

were prepared via *in situ* formation of compound [**1**] and subsequent addition of silver hexafluoridoantimonate or 8-quinolinol (Hquin), respectively (Scheme 3). All cobalt(III)-selenolate compounds were obtained in good yields (76 %, 91 %, 78 %, for [**2**], [**3**](SbF$_6$)$_2$, and [**4**]Cl, respectively), and appeared to be hygroscopic. The ESI-MS spectrum of an acetonitrile solution of [**2**] (Figure S7) shows peaks at *m/z* 464.0 and 889.0 attributed to the species $[Co(L^1Se)(NCS)(MeCN)]^+$ and $[2\times\mathbf{2} - 2SCN^- + HCOO^-]^+$, respectively. The ESI-MS spectrum of an acetonitrile solution of [**3**](SbF$_6$)$_2$ (Figure S8) shows peaks at *m/z* 223.6, 410.1, 863.0, and 1054.9, corresponding to the species $[\mathbf{3}]^{2+}$, $[\mathbf{3} - 2MeCN + HCOO^-]^+$, $[2\times\mathbf{3} - 4MeCN + 3HCOO^-]^+$, and $[2\times\mathbf{3} - 4MeCN + 2HCOO^- + (SbF_6)]^+$, respectively. The ESI-MS spectrum of an acetonitrile solution of compound [**4**]Cl (Figure S9) shows a major peak at *m/z* 509.1 which can be assigned to [**4**]$^+$. All cobalt(III)-selenolate compounds were found to be diamagnetic based on $^1$H-NMR spectroscopy (Figure S10–S16) and the determination of their magnetic moments using a magnetic susceptibility balance. Elemental analysis of the cobalt(III)-selenolate compounds show that the compounds were analytically pure (further details in Experimental Section).

## Single Crystal X-ray Crystallography

Single crystals of [**1**], [**2**], and [**4**]Cl were obtained using vapor diffusion of diethyl ether into solutions of each compound (See Experimental Section). Unfortunately, single crystals of compound [**3**](SbF$_6$)$_2$ could not be obtained as all crystallization attempts resulted in the formation of oils. Projections of the crystal structures are depicted in Figure 1. Full crystallographic parameters are provided in Table S1. Compound [**1**] crystallizes in the triclinic space group *P*-1 and the asymmetric unit contains one molecule of [**1**] and one lattice diethyl ether solvent molecule. Both cobalt(II) centers are found to be in a distorted trigonal-bipyramidal geometry ($\tau_5 = 0.72$ for Co1 and $\tau_5 = 0.62$ for Co2, $\tau_5 = 1$ is calculated for a perfect trigonal-bipyramidal geometry and $\tau_5 = 0$ for perfect square pyramidal geometry).[11] Each of the cobalt(II) centers is coordinated by three nitrogen atoms from the ligand $L^1SeSeL^1$ and two chloride anions. The apical positions are occupied by one of the chloride ions and the tertiary amine nitrogen atom. The diselenide group is not coordinated to the metal centers, as observed for the disulfide group in the related compound $[Co_2(L^1SSL^1)Cl_4]$.[5b]

Selected bond distances and angles are provided in Table 1. The Se1–Se2 bond distance (2.3208(7) Å) is in agreement with the average Se–Se bond length in reported structures (2.305 Å).[12] All other bond distances and angles are also within the expected values.

Compound [**2**] crystallizes in the orthorhombic space group *Pbca*, with one molecule of [**2**] in the asymmetric unit without co-crystallized lattice solvent molecules. The cobalt center is found in a near perfect octahedral geometry, formed by the coordination of five nitrogen atoms (two from NCS$^-$ ions and three from the ligand $L^1Se^-$) and one selenolate ion. The three nitrogen donors of the ligand $L^1Se^-$ are coordinated to the cobalt center in a meridional fashion, similar to the ligand $L^1S^-$ in previous reports.[5b,8] As a consequence, one of the NCS$^-$ ions is coordinated to *trans* to the selenolate ion and the other NCS$^-$ ion is coordinated *trans* to the tertiary amine nitrogen. The structure is very similar to the structure of the previously reported compound $[Co(L^1S)(NCS)_2]$.[5b] The distance between

**Table 1.** Selected bond distances and bond angles in [**1**].

| Atoms | Distance [Å] | Atoms | Bond angle [°] |
|---|---|---|---|
| Se1–Se2 | 2.3208(7) | N1–Co1–Cl2 | 165.89(10) |
| Co1–N1 | 2.303(3) | N1–Co1–Cl1 | 91.71(10) |
| Co1–N11 | 2.074(4) | N1–Co1–N11 | 75.99(13) |
| Co1–N21 | 2.079(4) | N1–Co1–N21 | 76.95(14) |
| Co1–Cl1 | 2.2848(13) | Cl2–Co1–Cl1 | 102.39(5) |
| Co1–Cl2 | 2.3290(12) | Cl2–Co1–N11 | 95.82(10) |
| | | Cl2–Co1–N21 | 97.52(11) |
| | | N11–Co1–Cl1 | 122.63(12) |
| | | N11–Co1–N21 | 118.18(15) |
| | | N21–Co1–Cl1 | 112.65(11) |

Research Article
doi.org/10.1002/ejic.202200445



**Table 2.** Bond distances and bond angles in [**2**].

| Atoms | Distance [Å] | Atoms | Bond angle [°] | Atoms | Bond angle [°] |
|---|---|---|---|---|---|
| Co1–Se1 | 2.3608(4) | Se1–Co1–N61 | 178.00(6) | N61–Co1–N51 | 89.65(8) |
| Co1–N1 | 1.9601(18) | Se1–Co1–N1 | 90.91(5) | N1–Co1–N11 | 84.87(7) |
| Co1–N11 | 1.9353(18) | Se1–Co1–N11 | 88.29(6) | N1–Co1–N21 | 84.20(7) |
| Co1–N21 | 1.9229(18) | Se1–Co1–N21 | 91.95(5) | N1–Co1–N51 | 179.27(8) |
| Co1–N51 | 1.8999(19) | Se1–Co1–N51 | 88.36(6) | N51–Co1–N11 | 95.14(8) |
| Co1–N61 | 1.9976(19) | N61–Co1–N1 | 91.08(7) | N51–Co1–N21 | 95.79(8) |
| | | N61–Co1–N11 | 91.78(8) | N11–Co1–N21 | 169.07(8) |
| | | N61–Co1–N21 | 88.35(7) | | |

**Table 3.** Bond distances and bond angles in [**4**]Cl.

| Atoms | Distance [Å] | Atoms | Bond angle [°] | Atoms | Bond angle [°] |
|---|---|---|---|---|---|
| Co1–Se1 | 2.3552(3) | Se1–Co1–O1 | 176.94(5) | O1–Co1–N31 | 85.47(7) |
| Co1–N1 | 1.9527(18) | Se1–Co1–N1 | 90.72(5) | N1–Co1–N11 | 83.81(8) |
| Co1–N11 | 1.9389(18) | Se1–Co1–N11 | 92.80(5) | N1–Co1–N21 | 85.48(8) |
| Co1–N21 | 1.9333(19) | Se1–Co1–N21 | 88.21(5) | N1–Co1–N31 | 174.67(7) |
| Co1–N31 | 1.9307(18) | Se1–Co1–N31 | 94.37(5) | N31–Co1–N11 | 94.37(8) |
| Co1–O1 | 1.9770(14) | O1–Co1–N1 | 89.53(7) | N31–Co1–N21 | 96.22(8) |
| | | O1–Co1–N11 | 90.26(7) | N11–Co1–N21 | 169.26(8) |
| | | O1–Co1–N21 | 88.77(7) | | |

Co1 and N61 ($NCS^-$ coordinated *trans* to Se) is slightly elongated (1.9976(19) Å) compared to the distance between Co1 and N51 (1.8999(19) Å), most likely due to the *trans* effect exerted by the selenolate ion. π-Stacking interactions are present between pyridines of two neighboring molecules, the distances ranging from 3.337 Å to 3.351 Å. Short contacts of 3.693 Å are present in the unit cell between the selenolate ion and a sulfur atom of an $NCS^-$ group of a neighboring molecule. A selection of bond distances and angles in [**2**] is provided in Table 2.

Compound [**4**]Cl crystallizes in the monoclinic space group $P2_1/n$, and the asymmetric unit contains one molecule of [**4**]Cl and two disordered lattice chloroform molecules. The cobalt center is found in a slightly distorted octahedral geometry, similar to [**2**].

Four nitrogen donor atoms (three from the ligand $L^1Se^-$, one from the ligand $quin^-$), one oxygen, and one selenolate donor atom are coordinated to the cobalt center. The structure of [**4**]Cl is very similar to the reported structure of its sulfur analog [Co($L^1$S)(quin)]Cl.[9] The bond distances and bond angles are similar to the structure [Co($L^1$S)(quin)]Cl, except for the Co1–Se1 bond distance, which is larger due to the larger ionic radius of selenium. Unlike [**2**], π-stacking interactions are not present in the structure of [**4**]Cl. A selection of bond distances and angles is provided in Table 3.

## Solution Studies of the Cobalt(II)-Diselenide and Cobalt(III)-Selenolate Compounds

The cobalt compounds described in this work are soluble in acetonitrile, except for [**2**] which is only slightly soluble in acetonitrile but fully soluble in dimethylsulfoxide. The UV-visible spectra of the compounds are provided in Figure 2. The UV-visible spectrum of the intense purple solution of [**1**] in acetonitrile shows two absorbances at 558 nm ($\varepsilon = 3.2 \times 10^2\ M^{-1}\,cm^{-1}$) and 635 nm ($\varepsilon = 2.2 \times 10^2\ M^{-1}\,cm^{-1}$) as well as a small peak at around 850 nm, corresponding to the Co(II) *d-d* transitions in a trigonal-bipyramidal geometry.[13] The UV-visible spectrum of [**1**] is very similar to that of the disulfide compound [$Co_2(L^1SSL^1)Cl_4$] reported earlier, with no apparent shift in the absorption wavelengths.[5b]

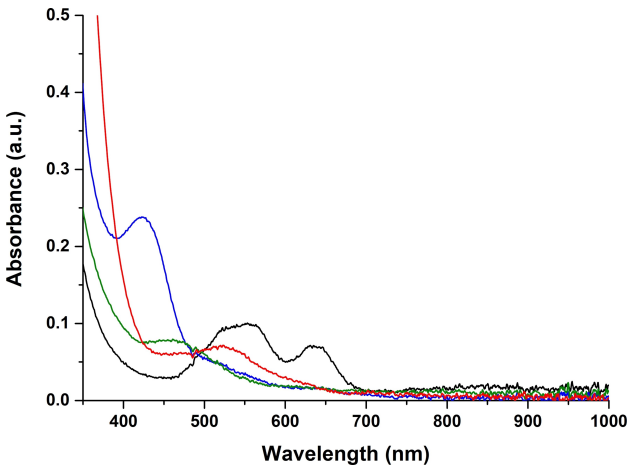


**Figure 2.** UV-visible spectra of acetonitrile solutions of [**1**] (2.5 mM concentration, black trace), [**3**]($SbF_6$)$_2$ (2 mM, green trace), [**4**]Cl (1 mM, blue trace), and a solution of [**2**] (2.5 mM, red trace) in 19:1 v:v acetonitrile:dimethylsulfoxide. UV-visible spectra were taken using a transmission dip probe with path length of 1.4 mm.

Compound [**2**] was dissolved in a mixture of acetonitrile: dimethylsulfoxide (19:1 v:v), resulting in a maroon-colored solution, whereas solutions of [**3**]($SbF_6$)$_2$ and [**4**]Cl in acetonitrile are yellow. The color of the solution of [**4**]Cl is rather intense compared to those of the two other cobalt(III)-selenolate compounds. The UV-visible spectra of cobalt(III)-selenolate compounds [**2**], [**3**]($SbF_6$)$_2$, and [**4**]Cl generally show one

Research Article
doi.org/10.1002/ejic.202200445



absorption peak. The UV-visible spectrum of [**2**] shows a weak absorption peak at 523 nm ($\varepsilon = 2.1 \times 10^2\ M^{-1}\ cm^{-1}$), whereas [**3**]$(SbF_6)_2$ shows a similar weak absorption at 465 nm ($\varepsilon = 3.4 \times 10^2\ M^{-1}\ cm^{-1}$). Such absorptions in UV-Vis spectra have been ascribed to Co(III) *d-d* transitions in a distorted octahedral geometry.[14] In comparison, the spectra of the Co(III)-thiolate analogs $[Co(L^1S)(NCS)_2]$ and $[Co(L^1S)(CH_3CN)_2]^{2+}$ in acetonitrile are slightly blue-shifted, with absorption peaks at 515 nm and 441 nm, for $[Co(L^1S)(NCS)_2]$ and $[Co(L^1S)(CH_3CN)_2]^{2+}$ respectively.[5b] The spectrum of [**4**]Cl shows one strong absorption peak at 422 nm ($\varepsilon = 1.7 \times 10^3\ M^{-1}\ cm^{-1}$) tentatively ascribed to a ligand-to-metal charge transfer from the $quin^-$ ligand to the cobalt center, similar to the spectrum of $[Co(L^1S)quin]Cl$.[9] However, the absorption peak for $[Co(L^1S)quin]Cl$ is slightly blue-shifted (at 412 nm) compared to that of [**4**]Cl.[9]

## DFT Studies: The Ligand-Field Splitting Energy of Selenolate Compounds

The ligand-field strength of exogenous ligands has been shown to affect the conversion of cobalt(II)-disulfide to cobalt(III)-thiolate species; the ligand-field splitting energy was estimated from the MO energy levels using DFT computations.[8] A similar approach was taken to approximate the ligand-field strength of the ligand $L^1SeSeL^1$ in this manuscript. The structures of [**2**], $[\mathbf{3}]^{2+}$, as well as $[\mathbf{4}]^+$ were optimized using ZORA-OPBE/TZP all-electron basis set. The equilibrium geometries show satisfactory results, as shown by similarities of the bond lengths of [**2**] and $[\mathbf{4}]^+$ with the experimental values from the crystal structures (Table 4). The calculated bond lengths deviate by 0.002 Å to 0.024 Å, the largest deviation of 0.024 Å concerns the Co1–N11 bond in $[\mathbf{2}]^+$.

**Table 4.** Comparison between experimental and DFT bond distances in [**2**] and in $[\mathbf{4}]^+$.

| Atoms | Bond distance in [**2**] [Å] | | Atoms | Bond distance in $[\mathbf{4}]^+$ [Å] | |
|---|---|---|---|---|---|
| | XRD | DFT | | XRD | DFT |
| Co1–Se1 | 2.3608(4) | 2.358 | Co1–Se1 | 2.3552(3) | 2.361 |
| Co1–N1 | 1.9601(18) | 1.966 | Co1–N1 | 1.9527(18) | 1.967 |
| Co1–N11 | 1.9353(18) | 1.911 | Co1–N11 | 1.9389(18) | 1.925 |
| Co1–N21 | 1.9229(18) | 1.906 | Co1–N21 | 1.9333(19) | 1.925 |
| Co1–N51 | 1.8999(19) | 1.846 | Co1–N31 | 1.9307(18) | 1.921 |
| Co1–N61 | 1.9976(19) | 1.962 | Co1–O1 | 1.9770(14) | 1.958 |

The five non-degenerate molecular orbitals were selected with the highest contribution from Co *d*-orbitals (Figure S17–S19). These five orbitals approximately form two sets of orbitals in agreement with an octahedral splitting according to ligand-field theory. As the two sets of orbitals also contain contributions from the ligands in varying amounts, the *d*-orbital splitting energy can only be estimated in a rather qualitative way from the energy difference of the highest and the lowest orbital of this set. The results are shown in Figure 3 and compared to the sulfur analogs of [**2**], $[\mathbf{3}]^{2+}$, and $[\mathbf{4}]^+$. The energy differences between the highest and lowest MO with large *d*-orbital contributions in compounds [**2**], $[\mathbf{3}]^{2+}$, and $[\mathbf{4}]^+$ are qualitatively smaller than those of their corresponding sulfur analogs. Therefore, replacement of sulfur with selenium apparently resulted in a slightly smaller ligand-field strength of the $L^1Se^-$ ligand. The differences between the *d*-orbital energies of the selenolate compounds with those of the sulfur analogs seems to follow a trend, i.e. the difference in energy of the highest and lowest MO comprising major *d*-orbital contribution between the Se and S compounds becomes smaller from [**2**] via $[\mathbf{3}]^{2+}$ to $[\mathbf{4}]^+$. This apparent trend seems to be related to the ligand-field strength of the auxiliary ligands, from the weakest to the strongest in the order of $NCS^- < CH_3CN < quin^-$, indicating that the contribution of the auxiliary ligand in the overall ligand-field splitting energy becomes dominant.[15]

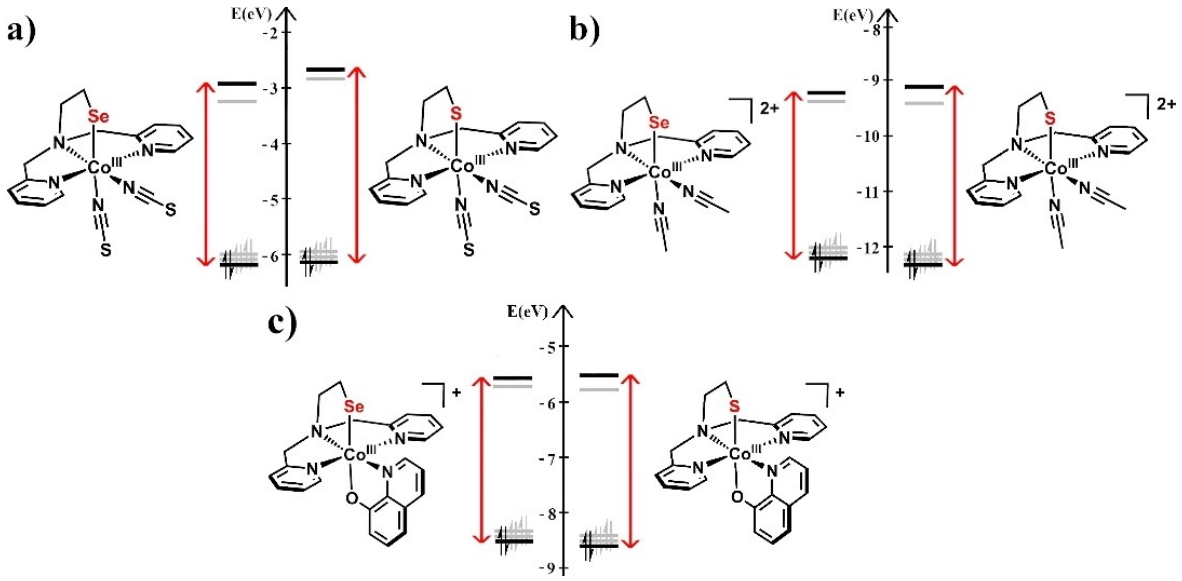


**Figure 3.** Comparison of the estimated *d*-orbital splitting energies of a) [**2**], b) $[\mathbf{3}]^{2+}$, and c) $[\mathbf{4}]^+$ with their corresponding sulfur analogues.

Research Article
doi.org/10.1002/ejic.202200445



## Discussion

The disulfide ligand $L^1SSL^1$ in copper(I) or cobalt(II) complexes has been reported to facilitate intramolecular electron transfer with the metal center, in a so-called redox-conversion reaction.[5b,16] To the best of our knowledge, this redox-conversion reaction has never been reported for a selenium-based ligand. Therefore, our study of the potential redox-conversion of cobalt(II)-diselenide compounds started with the preparation of the new ligand $L^1SeSeL^1$, which structurally resembles the sulfur analog $L^1SSL^1$. Our results show that indeed redox-conversion reactions can also take place using this diselenide ligand.

The reaction of $L^1SeSeL^1$ with cobalt(II) chloride in acetonitrile afforded the cobalt(II)-diselenide compound [**1**], which resembles the reported compound $[Co_2(L^1SSL^1)Cl_4]$, having very similar spectroscopic properties.[5b] The reaction with cobalt(II) thiocyanate resulted in the cobalt(III)-selenolate complex [**2**], similar to $[Co(L^1S)(NCS)_2]$.[5b] However, the ESI-MS spectrum of a solution of [**2**] (Figure S7) shows signals attributed to the apparent redox conversion to the diselenide dimer of the compound. In the solid state [**2**] is pure, and despite its low solubility, the $^1$H-NMR spectrum shows that compound [**2**] is stable in $CD_3CN$.

Like its sulfur analog, [**1**] undergoes a redox-conversion reaction upon the addition of an external trigger, as shown by the formation of [**3**]$(SbF_6)_2$ and [**4**]Cl after treatment of *in situ* formed [**1**] with a silver salt or quinolinol. Full conversion of [**1**] to [**3**]$(SbF_6)_2$ was achieved successfully. In principle, this reactivity is similar to the formation of $[Co(L^1S)(MeCN)_2]^{2+}$ from a reaction of $L^1SSL^1$ with $[Co(MeCN)_6](BF_4)_2$,[5b] or from the dissolution of $[Co_2(L^1SSL^1)(PF_2O_2)_2](PF_6)_2$ in acetonitrile.[6] Acetonitrile will coordinate to the cobalt center and has sufficiently strong ligand-field effect to trigger the conversion to the cobalt(III) isomer, as long as there is no competition of a strongly coordinating ligand or anion. Despite the successful formation of [**3**]$(SbF_6)_2$, this compound appeared to be unstable in solution. Partial decomposition of the cobalt(III)-selenolate complex is indicated in the $^1$H-NMR spectrum of [**3**]$(SbF_6)_2$ by the presence of several peaks in the aromatic region (6.60–7.25 ppm) as well as at 2.75 ppm, which possibly arise from degradation of the ligand. Full conversion of [**1**] to [**4**]Cl was achieved in a clean manner with the strong-field ligand quinolinolate.

It seems that the presence of selenium in the ligand causes a smaller ligand-field splitting, as evidenced by the red shifts of the UV-visible absorption peaks relative to those of the sulfur analogs and based on our computational results. Although the ligand-field splitting energy of the selenium-based ligand may be smaller than that of the sulfur analog, it appears that this can be counteracted by the auxiliary ligand. This assumption is supported by our DFT computations: the difference in energy of the highest and lowest molecular orbital with major *d*-orbital contribution of the selenolate compounds compared to the thiolate analogs becomes smaller in the order of $NCS^-$, $CH_3CN$, and $quin^-$. These results indicate that indeed the ligand-field strength contribution of these auxiliary ligand overcomes the smaller ligand-field splitting energy of the selenium donor atom.

Generally, our results reveal the similarities and differences in redox-conversion reactivity of the diselenide ligand $L^1SeSeL^1$ compared to that of $L^1SSL^1$. The relative instability of the cobalt(III)-selenolate compounds can be explained by the more negative reduction potential of the diselenide bond than that of the disulfide bond.[17] Re-oxidation of selenolate to the diselenide (dimer) appears to be relatively easy as indicated by the presence of peaks assigned to dimeric compounds in the ESI-MS spectra of [**2**] and [**3**]$(SbF_6)_2$, in agreement with the calculated smaller ligand-field splitting energy. It appears that the incorporation of selenium in the ligand, and the combination with external ligands that exert small ligand-field splitting causes the redox-conversion reaction to be more at equilibrium rather than in one of the extremes of the redox isomers.

## Conclusion

The diselenide analog $L^1SeSeL^1$of the disulfide ligand $L^1SSL^1$ was successfully synthesized. Reaction of the ligand $L^1SeSeL^1$ with cobalt(II) salts resulted in the formation of either cobalt(II)-diselenide compound [**1**] with chloride ions or the cobalt(III)-selenolate compound [**2**] with thiocyanate ions. The redox-conversion of cobalt(II)-diselenide compound [**1**] to cobalt(III)-selenolate compounds [**3**]$(SbF_6)_2$ or [**4**] was successful, using the strategies employed for $L^1SSL^1$. The cobalt(III)-selenolate compounds [**2**] and [**3**]$(SbF_6)_2$ appear to be relatively unstable in solution, the compounds partially revert to a diselenide compound or decompose. However, formation of [**4**] is clean, showing that the ligand-field strength of the auxiliary ligand can overpower the weaker ligand-field exerted by the selenium-based ligand. Overall, our results indicate that cobalt compounds with the ligand $L^1SeSeL^1$ show reactivity that is very similar to the sulfur analogs. The selenium-based ligand appears to exert a slightly lower ligand-field strength, which is not unexpected due to the stronger pi-donating effects of the larger lone pairs on selenium. These studies can be directed to investigate the kinetics of the reaction, or derivatization of the ligand $L^1SeSeL^1$, which may give insights not only in the diselenide to selenolate conversion, but also their efficiency in natural systems.

## Experimental Section

### General

All reagents were purchased from commercial sources and used as received unless noted otherwise. Deoxygenated solvents used were obtained by the freeze-pump-thaw method followed by drying the solvents using appropriate size of molecular sieves. The synthesis of the cobalt compounds was performed using standard Schlenk-line techniques under argon atmosphere. $^1$H-NMR spectra were recorded on a Bruker 300 DPX spectrometer at room temperature. Mass spectra were recorded on a Thermo Scientific MSQ Plus or Shimadzu LCMS 2020 mass spectrometer with electrospray ioniza-

tion (ESI) method, formic acid was added to the eluting solvent with 1% final concentration. Simulated mass spectra were generated using the mMass (version 5.5.0) software.[18] IR spectra were obtained using a PerkinElmer Spectrum Two System equipped with Universal ATR module containing diamond crystal for single reflection (scan range 400–4000 $cm^{-1}$, resolution 4 $cm^{-1}$). Analyses of bond distances and angles of the structures were performed using the Mogul module in Mercury (version 4.3.1) software.[19] UV-visible spectra were collected using a transmission dip probe with variable path lengths and reflection probe on an Avantes AvaSpec-2048 spectrometer and using an Avalight-DH-S-Bal light source. Elemental analyses were performed by the Microanalytical Laboratory Kolbe in Germany.

### Single crystal X-ray crystallography

All reflection intensities were measured at 110(2) K using a SuperNova diffractometer (equipped with Atlas detector) with Mo $K\alpha$ radiation ($\lambda = 0.71073$ Å) under the program CrysAlisPro (Version CrysAlisPro 1.171.39.29c, Rigaku OD, 2017). The same program was used to refine the cell dimensions and for data reduction. The structure was solved with the program SHELXS-2018/3 and was refined on $F^2$ with SHELXL-2018/3.[20] Numerical absorption correction based on Gaussian integration over a multifaceted crystal model was applied using CrysAlisPro. The temperature of the data collection was controlled using the system Cryojet (manufactured by Oxford Instruments). The H atoms were placed at calculated positions using the instructions AFIX 23, AFIX 43 or AFIX 137 with isotropic displacement parameters having values 1.2 or 1.5 $U_{eq}$ of the attached C atoms. The crystal structures of [**1**] and [**2**] are ordered. For compound [**4**]Cl, the two lattice chloroform molecules were found to be disordered over either two or three orientations; the occupancy factors of the major / minor components of the disorder can be retrieved from the .cif file.

### Computational methods

All calculations were performed with density functional theory using the Amsterdam Density Functional (ADF) program version 2017.103.[21] Geometries and energies were computed using OPBE functional.[22] Molecular orbitals (MO) were expanded in a large uncontracted TZP Slater type orbital (STO) basis set.[23] Scalar relativistic effects were accounted for using the zeroth order regular approximation (ZORA).[24] The stationary points were checked to be minima at potential energy surface using vibrational analysis. The calculations for all cobalt(III)-selenolate compounds were done with $S = 0$ (low-spin cobalt(III) center). The *d*-orbital splitting energies were estimated using similar method described in previous report.[8]

### Synthesis of the compounds

#### *Selenocystamine dihydrochloride ($C_4H_{12}N_2Se_2{\cdot}2HCl$)*

*Caution: Selenium and its derivative listed here are extremely toxic and exude a foul smell; one should ensure proper ventilation and personal protective equipment at all times.*

A 3-necked round-bottomed flask was purged with argon before the reaction was started. Into the 3-necked round-bottomed flask, selenium powder (4.75 g, 60.2 mmol) was added, followed by 25 mL of demineralized water (previously bubbled with argon). The flask was then fitted with a gas outlet and an addition funnel. In another flask, 15.0 grams of lead(II) acetate trihydrate was dissolved in 300 mL demineralized water. The solution of lead(II) acetate was added to a gas washing bottle, keeping the solution level above the bubbler to detect any gas formation. The gas outlet of the reaction flask was connected to the inlet of the gas washing bottle. In a separate flask, 4.54 grams of $NaBH_4$ (120 mmol, 2 equiv.) was dissolved in 25 mL demineralized water, bubbled with argon for 20 minutes, and the solution was quickly transferred to the addition funnel. The colloidal selenium mixture was stirred and $NaBH_4$ was added slowly to keep the bubbling at a moderate pace. During the addition of $NaBH_4$, the solution in the gas-trap apparatus changed color from colorless to black, indicating the formation of PbSe species. The grey colloidal selenium mixture changed to a clear red solution during the addition of $NaBH_4$ and ultimately to a light yellow solution after full addition of $NaBH_4$. The solution was stirred for 10 minutes, followed by addition of selenium powder (4.75 g, 60.2 mmol) in four portions over the course of 30 minutes. The resulting dark red-colored solution was stirred for another 20 minutes. While stirring, 2-chloroethylamine hydrochloride (13.9 g, 120 mmol, 2 equiv.) was dissolved in 30 mL NaOH 5 M, which was deoxygenated by bubbling with argon for 20 minutes. This solution was transferred to the addition funnel, then added dropwise to the reaction mixture. The gas outlet and the addition funnel was removed after the addition, and the resulting solution was stirred overnight at room temperature under an argon atmosphere.

The reaction mixture was transferred into a separating funnel, then extracted with $5 \times 100$ mL $CHCl_3$. The organic layer was collected and subsequently dried over $MgSO_4$. The organic layer was filtered and concentrated using a rotary evaporator. The resulting oil (15.34 g) was dissolved in 100 mL methanol and 100 mL ethyl acetate. Anhydrous HCl in diethyl ether (65 mL) was added slowly to the solution, and the reaction mixture was stirred for an hour. After an hour, the mixture was concentrated using a rotary evaporator. The resulting solid (12.13 g) was dissolved in the minimum amount of methanol, and ethyl acetate was added slowly until the formation of precipitates occurred. Filtration of the light yellow solid and subsequent washing with diethyl ether followed by drying in air gave a light yellow powder as the product. Yield = 7.05 g, (37%). ESI-MS found (calc.) for $[M+H]^+$ *m/z* 248.9 (248.94). $^1$H-NMR (300 MHz, $(CD_3)_2SO$, RT), δ(ppm): 8.24 (s, 4H, amine N**H**$_2$), 3.35 (s, 8H, $NH_2$-C**H**$_2$-C**H**$_2$-Se-).

#### *2,2′-Diselanediylbis(N,N-bis(pyridin-2-ylmethyl)ethan-1-amine) ($L^1SeSeL^1$)*

In a 500 mL round-bottom flask, selenocystamine dihydrochloride (3.22 grams, 10.1 mmol) was dissolved in 150 mL methanol, resulting in a red-colored solution. Into the solution, 2-pyridinecarboxaldehyde (4.0 mL, 42 mmol, 4 equiv.) was added and the reaction mixture was stirred for one hour. Then, sodium cyanoborohydride (2.95 g, 47.0 mmol, 4.7 equiv.) was added in four portions, the first two portions were added over the course of 15 minutes. The remaining portions were added after stirring the solution for 12 hours, over the course of 15 minutes. The color of the solution turned yellow-green, and the solution was stirred for another three days. The reaction was quenched after three days by addition of 37% HCl until pH = 1. The solvent was removed using a rotary evaporator, resulting in a yellow oil, which was dissolved in 50 mL NaOH (10 M). The solution was transferred into a separatory funnel and extracted with $3 \times 100$ mL $CHCl_3$. The organic layer was collected, dried over $MgSO_4$. Filtration of the solids and removal of the solvent using a rotary evaporator resulted in a red-orange oil, which was carefully treated with 10 mL 70% $HClO_4$. Absolute ethanol (400 mL) was added to the mixture, the initially formed turbid solution turned clear orange after 3 hours of stirring. The orange-colored solution was then removed, resulting in a dark red

sticky oil, which was converted back to the free base using 50 mL NaOH (10 M). The solution was transferred to a separatory funnel and extracted again with 3×100 mL $CHCl_3$. The organic layer was collected, dried over $MgSO_4$, filtered, and then the solvent was removed using a rotary evaporator. The resulting crude product (red oil) was crystallized using 300 mL petroleum ether under overnight reflux condition. After reflux, the petroleum ether solution was transferred to an erlenmeyer flask and stored in a refrigerator for several days until a pale red precipitate formed. The solids were collected by filtration, dried in air and weighed. Yield = 1.60 g (26%). ESI-MS found (calc.) for $[L^1SeSeL^1+H]^+$ *m/z* 612.9 (613.1) $[L^1SeSeL^1+2H]^{2+}$ *m/z* 306.8 (307.06). $^1$H-NMR (300 MHz, $CD_3CN$, RT), δ(ppm): 2.79–2.84 (t, 4H, N-$CH_2$-C**H**$_2$-Se), 3.04–3.08 (t, 4H, N-C**H**$_2$-$CH_2$-Se), 3.78 (s, 8H, N-C**H**$_2$-Py), 7.17–7.22 (ddd, 4H, Py-**H**$_5$), 7.54–7.56 (d, 4H, Py-**H**$_3$), 7.68–7.74 (td, 4H, Py-**H**$_4$), 8.46–8.49 (m, 4H, Py-**H**$_6$). Elemental analysis (%) for $L^1SeSeL^1$ ($C_{28}H_{32}N_6Se_2$) calcd. C, 55.09; H, 5.28; N, 13.77; found C, 54.96; H, 5.31; N, 13.60.

### *[$Co_2$($L^1SeSeL^1$)($Cl)_4$] ([1])*

The ligand $L^1SeSeL^1$ (65.8 mg, 0.108 mmol) was dissolved in 5 mL dry and deoxygenated acetonitrile. Anhydrous $CoCl_2$ (28.0 mg, 0.216 mmol, 2 equiv.) was added into the solution of $L^1SeSeL^1$ and the color immediately turned dark purple. The solution was stirred for three hours and then concentrated *in vacuo* until approximately 1 mL was left in the flask. Diethyl ether (12 mL) was subsequently added into the flask, affording a purple precipitate. The precipitate was filtered, washed twice with diethyl ether, then dried *in vacuo*. The dried purple powder was collected and weighed. The purple powder is air stable. Yield = 46.6 mg (50%). Purple platelike single crystals of [**1**] were grown using vapor diffusion of diethyl ether into an acetonitrile solution of [**1**]. IR (neat, $cm^{-1}$): 3065vw, 3029vw, 2964vw, 2916w, 2848vw, 1606vs, 1571 m, 1480s, 1442vs, 1380w, 1367w, 1308 m, 1292 m, 1260 m, 1226vw, 1156 m, 1099 m, 1083 m, 1053 s, 1023vs, 981w, 961 m, 900w, 862w, 844w, 766vs, 736 m, 683w, 649 m, 513w, 477 m, 417 s. ESI-MS found (calc.) for $[\mathbf{1}-2Cl^-]^{2+}$ m/z 400.0 (399.95), for $[\mathbf{1}-2Cl^-+HCOO^-]^+$ *m/z* 845.1 (844.90). Elemental analysis (%) for [**1**] ($C_{28}H_{32}Co_2N_6Se_2Cl_4$) calcd. C, 38.65; H, 3.71; N, 9.66; found C, 38.49; H, 3.69; N, 9.46.

### *[Co($L^1Se$)($NCS)_2$] ([2])*

Preparation of [**2**] was similar to compound [**1**], using $Co(SCN)_2$ instead of $CoCl_2$. Ligand $L^1SeSeL^1$ (68.0 mg, 0.111 mmol) in dry and deoxygenated acetone was mixed with $Co(SCN)_2$ (39.0 mg, 0.222 mmol, 2 equiv.). A purple powder was obtained. Yield = 81.0 mg (76%). Dark red single crystals of [**2**] were grown using vapor diffusion of diethyl ether into a 1:1 acetonitrile:methanol solution of [**2**] over the course of three days. IR (neat, $cm^{-1}$): 2969w, 2900w, 2057vs, 1692w, 1606 s, 1572 m, 1482 m, 1443 s, 1366 m, 1307 m, 1291 m, 1250 m, 1225w, 1155 m, 1100 m, 1079 m, 1054 s, 1024 s, 973 m, 957 m, 901w, 862w, 841w, 763vs, 734 m, 722 m, 650 m, 512w, 475 s, 446w, 418 s. $^1$H-NMR (300 MHz, $CD_3CN$, RT), δ(ppm): 3.22–3.30 (m, 2H, N-C**H**$_2$-$CH_2$-Se), 4.18–4.24 (d, 2H, N-C**H**$_2$-py), 4.92–4.97 (d, 2H, N-C**H**$_2$-py), 7.44–7.47 (d, 2H, Py-**H**$_3$), 7.54–7.59 (t, 2H, Py-**H**$_5$), 7.96–8.01 (t, 2H, Py-**H**$_4$), 8.47–8.49 (d, 2H, Py-**H**$_6$), the proton signal of N-$CH_2$-C**H**$_2$-Se is obscured by the solvent peak at around 2.12–2.25 ppm, but was assigned using $^1$H-COSY spectrum. ESI-MS found (calc.) for $[\mathbf{2}-SCN^- + MeCN]^+$ *m/z* 463.9 (463.99), for $[2\times\mathbf{2}-2SCN^-+HCOO^-]^+$ *m/z* 889.0 (888.92). Elemental analysis (%) for [**2**] ($C_{16}H_{16}CoN_5S_2Se$) calcd. C, 40.01; H, 3.36; N, 14.58; found C, 39.46; H, 3.31; N, 14.31.

### *[Co($L^1Se$)($MeCN)_2$]($SbF_6)_2$ ([3]($SbF_6)_2$)*

The ligand $L^1SeSeL^1$ (61.0 mg, 0.100 mmol) was dissolved in 5 mL dry and deoxygenated acetonitrile. Anhydrous $CoCl_2$ (26.0 mg, 0.200 mmol, 2 equiv.) was added and the resulting, purple-colored solution was stirred for 30 minutes. Silver hexafluoridoantimonate (143.7 mg, 0.418 mmol, 4.18 equiv.) was added and the resulting solution turned brown with some white precipitate, presumably AgCl. The resulting suspension was stirred for 2 hours, followed by filtration into a clean Schlenk flask. The brown filtrate was concentrated until approximately 1 mL. Diethyl ether (12 mL) was added into the flask resulting in the formation of a dark brown oil. The oil was separated by careful removal of the diethyl ether using a syringe, then the oil was washed twice with diethyl ether, and dried *in vacuo*. The oil quickly solidified and turned into a semi-crystalline powder. Yield = 166.8 mg (91%). IR (neat, $cm^{-1}$): 3516 s, 3466 s, 3262 m, 3201 m, 3122 m, 2988 m, 2972 m, 2901 m, 1624 m, 1612 m, 1573w, 1538w, 1471 m, 1446 m, 1411w, 1394w, 1378w, 1290w, 1249w, 1231w, 1165w, 1056 m, 1026 m, 973w, 896vw, 880vw, 838w, 821vw, 765 s, 727 s, 655vs, 624vs, 480 m, 452 m, 421 m. ESI-MS found (calcd.) for $[\mathbf{3}]^{2+}$ *m/z* 223.6 (223.52), for $[\mathbf{3}-2MeCN+HCOO^-]^+$ *m/z* 410.1 (410.98), for a dimer $[2\times\mathbf{3}-4MeCN+3HCOO^-]^+$ *m/z* 863.0 (862.96), and for $[2\times\mathbf{3}-4MeCN+2HCOO^-+SbF_6^-]^+$ *m/z* 1054.9 (1054.86). $^1$H-NMR (300 MHz, $CD_3OD$, RT), δ(ppm): 2.83–2.86 (m, 2H, N-$CH_2$-C**H**$_2$-Se), 3.07–3.11 (m, 2H, N-C**H**$_2$-$CH_2$-Se), 3.81 (s, 4H, N-C**H**$_2$-py), 7.42-7.47 (t, 4H, Py-**H**$_3$ and Py-**H**$_5$), 7.85–7.91 (t, 2H, Py-**H**$_4$), 8.62–8.64 (d, 2H, Py-**H**$_6$),. The compound is not stable in solution, as is apparent from impurities detected at 2.75 (s, 1H), 6.38–6.44 (t, 0.5H), 6.72–6.75 (d, 0.5H), 6.89–6.91 (d, 0.5H), 7.19–7.24 (t, 0.5H). Elemental analysis (%) for [**3**]($SbF_6)_2$ ($C_{18}H_{22}CoF_{12}N_5Sb_2Se$) calcd. C, 55.09; H, 5.28; N, 13.77; found C, 54.96; H, 5.31; N, 13.60.

### *[Co($L^1Se$)(quin)]Cl ([4]Cl)*

The ligand $L^1SeSeL^1$ (61.2 mg, 0.100 mmol) and anhydrous $CoCl_2$ (26.0 mg, 0.200 mmol, 2 equiv.) were dissolved in 5 mL dry and deoxygenated methanol, affording a solution of [**1**] as described above. Into this solution, 8-quinolinol (28.9 mg, 0.200 mmol, 2 equiv.) was added. The solution turned from purple into brown and the solution was stirred for another three hours. The solution was concentrated until approximately 1 mL, diethyl ether (12 mL) was added to the concentrated solution, which resulted in the formation of a brown precipitate. The brown precipitate was filtered, washed twice with diethyl ether, then dried *in vacuo*, and weighed. Yield = 85.2 mg (78%). Dark brown single crystals of [**4**]Cl were grown using vapor diffusion of diethyl ether into a chloroform solution of [**4**]Cl. IR (neat, $cm^{-1}$): 3361b, 2984w, 2969w, 2050vw, 1657 s, 1632 s, 1571 m, 1498 s, 1463 s, 1408 s, 1374 s, 1321 s, 1284 m, 1222w, 1173w, 1156w, 1110 m, 1053w, 1008 m, 980w, 876w, 831 s, 803w, 749 s, 703 s, 663w, 643w, 552w, 531 m, 516w 501w, 454w, 420w. ESI-MS found (calcd.) for $[\mathbf{4}]^+$ *m/z* 509.1 (509.03) and its isotopic pattern. $^1$H-NMR (300 MHz, $CD_3CN$, RT), δ(ppm): 3.61–3.63 (t, 2H, N-C**H**$_2$-$CH_2$-Se), 4.54–4.59 and 5.45–5.50 (d, d, total 4H, N-C**H**$_2$-Py), 6.86–6.89 (dd, 1H, ortho-C**H**-O(quin)), 7.02–7.05 (dd, 1H, para-C**H**-O(quin)), 7.10–7.15 (t, 2H, Py-**H**$_5$), 7.34–7.39 (m, 3H, Py-**H**$_3$ and meta-C**H**-O(quin)), 7.46–7.49 (d, 2H, Py-**H**$_4$), 7.74 (dd, 1H, meta-C**H**-N(quin)), 7.79–7.85 (td, 2H, Py-**H**$_6$), 8.45–8.48 (d, 1H, para-C**H**-N(quin)), 9.02–9.04 (d, 1H, ortho-C**H**-N(quin)), the proton signal of N-$CH_2$-C**H**$_2$-Se is obscured by the solvent peak at around 2.15–2.25 ppm, but was assigned using $^1$H-COSY spectrum. Elemental analysis (%) for [**4**]Cl ($C_{23}H_{22}ClCoN_4OSe$) + 0.2 $CHCl_3$ calcd. C, 49.09; H, 3.94; N, 9.87; found C, 48.77; H, 3.97; N, 9.89.

Research Article
doi.org/10.1002/ejic.202200445



## Supporting Information

ESI-MS spectra, NMR spectra, detailed frontier orbital analyses of [**2**], $[\mathbf{3}]^{2+}$, and $[\mathbf{4}]^{+}$, table of crystallographic parameters for the crystal structures in the present work, and Cartesian coordinates of optimized structures are provided.

Deposition Numbers 2189395 ([**1**]), 2189396 ([**2**]), and 2189397 ([**4**]Cl) contain the supplementary crystallographic data for this paper. These data are provided free of charge by the joint Cambridge Crystallographic Data Centre and Fachinformationszentrum Karlsruhe Access Structures service www.ccdc.cam.ac.uk/structures.

## *Acknowledgements*

*We are grateful to Dr. Sipeng Zheng for the ESI-MS measurements.*

## *Conflict of Interest*

The authors declare no conflict of interest.

## Data Availability Statement

The data that support the findings of this study are available in the supplementary material of this article.

**Keywords:** Chalcogens · Cobalt · Density functional calculations · Redox chemistry · Selenium

[1] a) M. Gennari, C. Duboc, *Acc. Chem. Res.* **2020**, *53*, 2753–2761; b) C. Hu, Y. Yu, J. Wang, *Chem. Commun.* **2017**, *53*, 4173–4186; c) D. R. Martin, D. V. Matyushov, *Sci. Rep.* **2017**, *7*, 1–11.
[2] a) A. Bock, K. Forchhammer, J. Heider, W. Leinfelder, G. Sawers, B. Veprek, F. Zinoni, *Mol. Microbiol.* **1991**, *5*, 515–520; b) J. E. Cone, R. Martindelrio, J. N. Davis, T. C. Stadtman, *Proc. Natl. Acad. Sci. USA* **1976**, *73*, 2659–2663; c) T. Takei, T. Ando, T. Takao, Y. Ohnishi, G. Kurisu, M. Iwaoka, H. Hojo, *Chem. Commun.* **2020**, *56*, 14239–14242; d) H. J. Reich, R. J. Hondal, *ACS Chem. Biol.* **2016**, *11*, 821–841.
[3] D. Steinmann, T. Nauser, W. H. Koppenol, *J. Org. Chem.* **2010**, *75*, 6696–6699.
[4] R. E. Huber, R. S. Criddle, *Arch. Biochem. Biophys.* **1967**, *122*, 164–173.
[5] a) E. C. M. Ording-Wenker, M. van der Plas, M. A. Siegler, S. Bonnet, F. M. Bickelhaupt, C. Fonseca Guerra, E. Bouwman, *Inorg. Chem.* **2014**, *53*, 8494–8504; b) F. Jiang, M. A. Siegler, X. Sun, L. Jiang, C. Fonseca Guerra, E. Bouwman, *Inorg. Chem.* **2018**, *57*, 8796–8805.
[6] F. Jiang, C. Marvelous, A. C. Verschuur, M. A. Siegler, S. J. Teat, E. Bouwman, *Inorg. Chim. Acta* **2022**, *535*, 120880.
[7] M. Gennari, B. Gerey, N. Hall, J. Pecaut, M.-N. Collomb, M. Rouzieres, R. Clerac, M. Orio, C. Duboc, *Angew. Chem. Int. Ed.* **2014**, *53*, 5318–5321; *Angew. Chem.* **2014**, *126*, 5422–5425.
[8] C. Marvelous, L. de Azevedo Santos, M. A. Siegler, C. Fonseca Guerra, E. Bouwman, *Dalton Trans.* **2022**, *51*, 8046–8055.
[9] C. Marvelous, L. de Azevedo Santos, M. A. Siegler, C. Fonseca Guerra, E. Bouwman, *Dalton Trans.* **2022**, *51*, 11675–11684.
[10] D. Yue, G. Cheng, Y. He, Y. Nie, Q. Jiang, X. Cai, Z. Gu, *J. Mater. Chem. B* **2014**, *2*, 7210–7221.
[11] A. W. Addison, T. N. Rao, J. Reedijk, J. Vanrijn, G. C. Verschoor, *J. Chem. Soc. Dalton Trans.* **1984**, *7*, 1349–1356.
[12] a) P. Singh, H. B. Singh, R. J. Butcher, *J. Organomet. Chem.* **2018**, *876*, 1–9; b) D. Sureshkumar, T. Gunasundari, V. Saravanan, S. Chandrasekaran, *Tetrahedron Lett.* **2007**, *48*, 623–626.
[13] a) S. L.-F. Chan, T. L. Lam, C. Yang, J. Lai, B. Cao, Z. Zhou, Q. Zhu, *Polyhedron* **2017**, *125*, 156–163; b) S. S. Massoud, K. T. Broussard, F. A. Mautner, R. Vicente, M. K. Saha, I. Bernal, *Inorg. Chim. Acta* **2008**, *361*, 123–131.
[14] a) F. Basolo, *J. Am. Chem. Soc.* **1950**, *72*, 4393–4397; b) N. Matsuoka, *Bull. Chem. Soc. Jpn.* **1986**, *59*, 2151–2155.
[15] a) Y. Shimura, R. Tsuchida, *Bull. Chem. Soc. Jpn.* **1956**, *29*, 311–316; b) T. Ishii, S. Tsuboi, G. Sakane, M. Yamashita, B. K. Breedlove, *Dalton Trans.* **2009**, *4*, 680–687.
[16] a) S. Itoh, M. Nagagawa, S. Fukuzumi, *J. Am. Chem. Soc.* **2001**, *123*, 4087–4088; b) Y. Ueno, Y. Tachi, S. Itoh, *J. Am. Chem. Soc.* **2002**, *124*, 12428–12429.
[17] D. Besse, F. Siedler, T. Diercks, H. Kessler, L. Moroder, *Angew. Chem. Int. Ed.* **1997**, *36*, 883–885; *Angew. Chem.* **1997**, *109*, 915–917.
[18] M. Strohalm, mMass - Open Source Mass Spectrometry Tool, www.mmass.org.
[19] C. F. Macrae, I. Sovago, S. J. Cottrell, P. T. A. Galek, P. McCabe, E. Pidcock, M. Platings, G. P. Shields, J. S. Stevens, M. Towler, P. A. Wood, *J. Appl. Crystallogr.* **2020**, *53*, 226–235.
[20] G. M. Sheldrick, *Acta Crystallogr. Sect. A* **2008**, *64*, 112–122.
[21] ADF2017.107, SCM Theoretical Chemistry Vrije Universiteit: Amsterdam, The Netherlands, www.scm.com.
[22] M. Swart, A. W. Ehlers, K. Lammertsma, *Mol. Phys.* **2004**, *102*, 2467–2474.
[23] E. Van Lenthe, E. J. Baerends, *J. Comput. Chem.* **2003**, *24*, 1142–1156.
[24] E. Van Lenthe, E. J. Baerends, J. G. Snijders, *J. Chem. Phys.* **1994**, *101*, 9783–9792.

Manuscript received: July 12, 2022
Revised manuscript received: August 19, 2022

# RESEARCH ARTICLE

The first redox-conversion reaction is reported using a selenium-based ligand. Comparison of the results of selenium- and sulfur-based systems revealed that the ligand-field strength of selenium is smaller than that of sulfur, which possibly causes the cobalt(III)-selenolate compounds to be less stable.

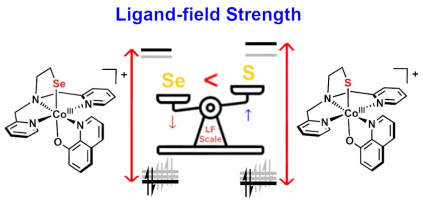


*Dr. C. Marvelous, Dr. L. de Azevedo Santos, Dr. M. A. Siegler, Prof. Dr. C. Fonseca Guerra*, Prof. Dr. E. Bouwman**



**Redox Conversion of Cobalt(II)-Diselenide to Cobalt(III)-Selenolate Compounds: Comparison with Their Sulfur Analogs**